Check for updates

Application of a novel definitive screening design to *in situ* chemical oxidation of acid orange-II dye by a Co^{2+}/PMS system

Chunyong Zhang, [iD] *[ab] Wei Chen,[a] Jiahui Xian[a] and Degang Fu[b]

In this work, a novel definitive screening design (DSD) was initially used to investigate the *in situ* chemical oxidation of acid orange-II (AO II) dye using a homogeneous cobalt-catalyzed peroxymonosulfate (Co^{2+}/PMS) system. Experiments were performed in a batch reactor using a synthetic AO II solution containing cobalt ions, humic acid (HA) and five electrolyte salts (NaCl, NaNO$_3$, NaHCO$_3$, Na$_2$SO$_4$ and NaH$_2$PO$_4$). The effects of nine operating variables on AO II degradation: NaCl concentration (0–20 mM), NaH$_2$PO$_4$ concentration (0–20 mM), NaHCO$_3$ concentration (0–20 mM), NaNO$_3$ concentration (0–20 mM), Na$_2$SO$_4$ concentration (0–20 mM), HA concentration (0–40 mg L^{-1}), PMS concentration (2–10 mM), AO II concentration (0–100 mg dm^{-3}) and Co^{2+} concentration (0–1.36 mM), were investigated. Analysis of a DSD model revealed that only four variables were statistically significant. Besides, our results indicated that there were no significant interactive effects between the five anions employed. Thereafter, a central composite rotatable design (CCRD) was adopted to further optimize these significant variables. A CCRD model describing AO II conversion as a function of PMS concentration, NaCl concentration and Co^{2+} concentration was then constructed and used to explore the final optimal operating conditions. As a consequence, the combination of DSD and CCRD allowed reducing the number of experiments from over 600 to only 39. Lastly, a plausible reaction sequence concerning the oxidation of AO II in the Co^{2+}/PMS/Cl$^-$ system was also proposed. The route of AO II oxidation involved hydroxylation and chlorination, signifying the roles of both sulfate radicals and active chlorine species.

1. Introduction

In situ chemical oxidation (ISCO) is an option that has been developed over the past decade to degrade various organic pollutants.[1] Specifically, a very recent process developed for ISCO involves the use of Co^{2+}-catalyzed peroxymonosulfate (Co^{2+}/PMS), which exhibits the advantages of excellent reactivity with contaminants and high longevity in the subsurface.[2] However, the performance of the process depends on multiple operating variables, such as anions, natural organic matter (NOM), solution pH, external energy (*e.g.*, UV light, electric field and ultrasound), *etc.*[3–5] For this reason, the traditional one-factor-at-a-time approach to optimization is time and regent extensive, and it is often unable to yield globally optimal operating conditions.

To overcome these limitations, the most common strategy is to employ statistical design methods, such as Box–Behnken design, Doehlert design and central composite rotatable design (CCRD).[6] Unfortunately, the number of experiments required

(NER) for these methods will increase exponentially with the number of variables tested.[7–9] For example, NER are 17, 36, 58, 100, 177, 324 and 635 for 3, 4, 5, 6, 7, 8 and 9-factor CCRD matrix, respectively. Thus, less than 5 variables should be employed in these designs. In case NER exceeds 5, statistical screening methods should be used to identify the significant variables while to exclude the insignificant ones.[10] The two-level Plackett–Burman design has been widely used for this purpose, but it is unable to capture interactive and pure-quadratic effects.[11] One solution to the problem is to adopt three-level screening designs. In this scenario, a novel three-level definitive screening design (DSD) has been recently developed by Jones and Nachtsheim.[12] The construction of DSD is achieved *via* a numerical algorithm that maximize the determinant of model matrix (of the main effect) while enforcing this structure. The rows of DSD are also randomly shuffled to create a random design. As a result, DSD allows all two-factor interactions and pure-quadratic effects to be examined with low level of aliasing.[13] Moreover, NER for *k*-factor DSD is only $2k + 1$ or $2k + 3$ (for an odd number of variables). Clearly, DSD is very promising for optimization of processes which involve a large number of operating variables.

However, a literature review claimed that only a few studies were devoted to the application of DSD in process

[a]Department of Chemistry, College of Science, Nanjing Agricultural University, Nanjing 210095, China. E-mail: zhangchy@njau.edu.cn; Fax: +86 25 84395207; Tel: +86 25 84395207

[b]State Key Laboratory of Bioelectronics, Southeast University, Nanjing 210096, China

This journal is © The Royal Society of Chemistry 2018

optimizations.[14–17] Thus, there is an urgent need to perform more validation studies so as to confirm its capability and adaptability in other experimental procedures.

In this contribution, the DSD approach was initially employed to investigate the oxidation reactions in homogeneous Co^{2+}/PMS system. Acid orange II (AO II) dye, a commercially azo dye with ideal molecule structure, was chosen as a pollutant model. The main objectives are: (1) to evaluate the suitability of DSD approach in optimizing the operating parameters of Co^{2+}/PMS system; (2) to identify the significant main and interaction effects involved in the reaction system; (3) to check the possible interactions between the five anions during the *in situ* chemical oxidations; and (4) to explore the oxidation pathway of AO II in Co^{2+}/PMS/NaCl system *via* quantum chemistry calculation and LC/MS technique. This study was novel, because nine variables of Co^{2+}/PMS system were initially included in a single experimental matrix. Specifically, an emphasis had been put on examining the influence of anions (Cl^-, $H_2PO_4^-$, HCO_3^-, NO_3^- and SO_4^{2-}). This was also the first investigation that examined the possible effects involved when five different anions were coexist in the reaction medium. For this reason, it was valuable to find that the work related to the effect of mixed salts was very significant. As expected, achieved results provided new insights into the reactions involved in homogeneous Co^{2+}/PMS system.

2. Experimental

2.1. Reagents and materials

Reagent-grade PMS from Aladdin (Shanghai, China), AO II, $CoSO_4$ (as Co^{2+} source), NaCl, Na_2SO_4, NaH_2PO_4, $NaHCO_3$, $NaNO_3$, $NaNO_2$ and humic acid (HA, in the form of sodium salt) from Wako (Japan), were used without purification. All stock solutions were carefully prepared with ultra-pure water.

2.2. Degradation procedure and analytical apparatus

Degradation experiments were performed in a 0.25 L sealed flask with a thermo regulated water bath. The processed solution volume was 0.10 L for each run. All degradation experiments were carried out in duplicate and average data were reported. For most entries, the samples were collected at 0 and 60 min after adding 10 mL 1.0 M $NaNO_2$ (as quenching reagent) into the reaction medium, so as to calculate the corresponding degradation percentage. The color decay of AO II was monitored by recording the spectrum from 200 to 800 nm using a Shimadzu UV-1800 spectrophotometer. Meanwhile, the mineralization of reaction medium was assessed with a Shimadzu TOC-L total organic carbon analyzer. Identification of the degraded products was achieved by the LC/MS analysis as described elsewhere (Waters Acquity UPLC/SQD analyzer, USA).[17]

2.3. Experiment design and analysis

According to the methodology of DSD, only important variables should be selected for the screening design. Hence, preliminary experiments were conducted and combined with a literature survey.[5,10] In the present work, nine operating variables of Co^{2+}/

Table 1 Factors with coded natural levels for the DSD

Factor/level	−1	0	+1	Unit
X_1: [NaCl]	0	10	20	mM
X_2: [NaH$_2$PO$_4$]	0	10	20	mM
X_3: [NaHCO$_3$]	0	10	20	mM
X_4: [NaNO$_3$]	0	10	20	mM
X_5: [Na$_2$SO$_4$]	0	10	20	mM
X_6: [HA]	0	20	40	mg dm^{-3}
X_7: [PMS]	2	6	10	mM
X_8: [AO II]	50	75	100	mg dm^{-3}
X_9: [Co^{2+}]	0	0.68	1.36	mM

PMS system had been chosen for the DSD matrix (see Table 1). Although solution pH was important for the system, it was not considered here because it might change the ionic form of the anions adopted (which was unfavorable for the investigation on the roles of anions). Another concern was, from the practical point of view, pH adjustment was not desirable due to the abundance of real dye wastewater and extra treatment costs involved. For each variable in DSD matrix, the operating levels for the three coded levels (−1, 0 and +1) were also given in Table 1. The variable levels were chosen by considering the limits of the experimental design, as well as by guaranteeing a proper distribution of the response factor (which played a vital role in determining the accuracy of DSD model). The 21 entries involved were randomly carried out to prevent biases.

After the significant variables had been identified, a classical five-level CCRD method was used to construct quadratic model which allowed oxidation performance to be quantified as a function of these variables.[18,19] The location of the optimum could then be easily determined by differentiation of the model. The data analyses were all performed using a JMP 10 software package (SAS, CARY, USA).

3. Results and discussions

3.1. Design of experiments: DSD and CCRD

The experimental design and the results of DSD obtained for color decay of AO II (Y_1, in mg L^{-1}) at reaction time of 60 min are presented in Table 2. Analysis of DSD data was carried out by forward stepwise regression and all subsets regression, as well as by determination of corrected Akaike Information Criterion (AICc) and Bayesian Information Criterion (BIC).[13] After elimination of insignificant effects, a simplified equation can be represented as:

$$Y_1 = b_0 + b_1X_1 + b_7X_7 + b_8X_8 + b_9X_9 + b_{89}X_8X_9 \qquad (1)$$

where Y_1 is the response, b_i and b_{ij} are the model coefficients, and X_i is the coded variable.

Table 3 presents the calculated model coefficients and related statistical results. Besides, the correlation coefficient (R^2) was equal to 0.905, the root mean square error (RMSE) was 19.3%, AICc was 205.01 and BIC was 206.43. Judging from these results, the DSD model obtained is deemed satisfactory from a statistical point of view.[12,13]

Table 2 Experimental design layout and observed response (Y_1, in mg dm^{-3}) for the DSD

Entry	X_1	X_2	X_3	X_4	X_5	X_6	X_7	X_8	X_9	Y_1
1	0	+1	+1	+1	+1	+1	+1	+1	+1	98.67
2	0	−1	−1	−1	−1	−1	−1	−1	−1	30.07
3	+1	0	−1	−1	−1	−1	+1	+1	+1	98.90
4	−1	0	+1	+1	+1	+1	−1	−1	−1	2.55
5	+1	−1	0	−1	+1	+1	−1	−1	+1	47.71
6	−1	+1	0	+1	−1	−1	+1	+1	−1	19.50
7	+1	−1	−1	0	+1	+1	+1	+1	−1	45.80
8	−1	+1	+1	0	−1	−1	−1	−1	+1	49.09
9	+1	−1	+1	+1	0	−1	−1	+1	−1	36.87
10	−1	+1	−1	−1	0	+1	+1	−1	+1	48.30
11	+1	−1	+1	+1	−1	0	+1	−1	+1	49.67
12	−1	+1	−1	−1	+1	0	−1	+1	−1	9.24
13	+1	+1	−1	+1	−1	+1	0	−1	−1	7.35
14	−1	−1	+1	−1	+1	−1	0	+1	+1	98.93
15	+1	+1	−1	+1	+1	−1	−1	0	+1	65.81
16	−1	−1	+1	−1	−1	+1	+1	0	−1	16.82
17	+1	+1	+1	−1	−1	+1	−1	+1	0	57.11
18	−1	−1	−1	+1	+1	−1	+1	−1	0	38.11
19	+1	+1	+1	−1	+1	−1	+1	−1	−1	49.71
20	−1	−1	−1	+1	−1	+1	−1	+1	+1	74.11
21	0	0	0	0	0	0	0	0	0	74.67

Table 3 Estimates of the model coefficients and the corresponding standard errors (SE), t-values and p-values

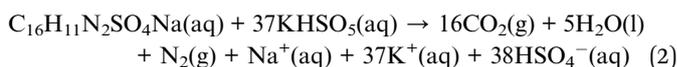| Coefficient	Term	Estimate	SE	t-Value	p-Value
b_0	Intercept	74.67	3.53	21.2	0.0301
b_1	[NaCl]	5.68	0.83	2.83	0.0426
b_7	[PMS]	5.16	0.83	2.60	0.0467
b_8	[AO II]	12.03	0.83	4.64	0.0418
b_9	[Co^{2+}]	22.96	0.83	5.97	0.0231
b_{89}	[AO II] × [Co^{2+}]	3.59	1.90	0.60	0.0004
b_2	[NaH$_2$PO$_4$]	−1.85	0.83	−2.20	0.2690
b_3	[NaHCO$_3$]	2.31	0.83	2.79	0.2194
b_4	[NaNO$_3$]	−2.56	0.83	−2.82	0.1460
b_5	[Na$_2$SO$_4$]	2.99	0.83	3.60	0.1725
b_6	[HA]	−2.92	0.83	−3.21	0.1067

To further check its accuracy, six extra entries have been performed. The experimental conditions, as well as the observed and predicted responses are presented in Table 4. By making comparisons between the response factors, the main and interaction effects involved may be easily identified. For

Table 4 Experimental conditions and results of the validation entries (X_2 to X_6 are all set at −1 level, Y(E) and Y(P) are the experimental and predicted responses, and PI refers the prediction intervals)

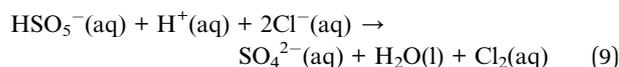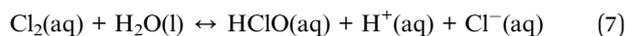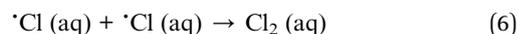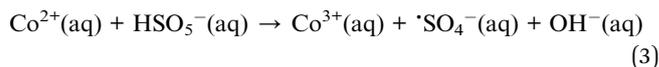| Entry	X_1	X_7	X_8	X_9	Y(E)	Y(P)	PI
1	−1	−1	0	0	55.08	63.83	27.03–100.63
2	+1	−1	0	0	63.56	75.19	38.39–111.99
3	−1	+1	0	0	63.34	74.15	37.35–110.95
4	+1	+1	0	0	72.52	85.51	48.71–122.31
5	+1	+1	−1	−1	35.33	54.11	17.31–90.91
6	+1	−1	+1	+1	98.38	124.09	87.29–160.89

example, the combined interaction effect of X_8 and X_9 is corrected predicted by comparing the responses of entries 5 and 6. Moreover, all experimental responses are fall within the corresponding 95% prediction intervals (PI), thus confirming the reliability of DSD model. As a result, the signs of main and interaction effects have been correctly predicted even if with the relatively low precision of screening experiments.

From Table 3 we also see that only four variables ([Co^{2+}], [AO II], [NaCl] and [PMS]) are statistically significant, and the order of significance is: [Co^{2+}] > [AO II] > [NaCl] > [PMS]. Moreover, [Co^{2+}] and [AO II] are involved in a significant two-way interaction. Specifically, the positive roles of [Co^{2+}] and [PMS] recorded are easy to understand since they are closely linked to the yields of oxidizing agents.[5] Interestingly, the positive role of [AO II] seems inconsistent with other observations in several previous works.[20,21] Here, assuming that the mineralization of AO II involves its conversion into CO$_2$ and N$_2$ as main inorganic byproducts (see eqn (2)),[22]

$$C_{16}H_{11}N_2SO_4Na(aq) + 37KHSO_5(aq) \rightarrow 16CO_2(g) + 5H_2O(l) + N_2(g) + Na^+(aq) + 37K^+(aq) + 38HSO_4^-(aq) \quad (2)$$

the [PMS] required for total mineralization of 100 mg dm^{-3} AO II (0.28 mM) is 10 mM. Interestingly, the [PMS] employed here (10 mM for +1 level) just guarantees the total mineralization of AO II (0.28 mM for +1 level). In other words, there are sufficient oxidants available in the reaction medium which can be utilized to oxidize the pollutant. In such cases, increasing initial substrate concentration ([AO II]) surely results in higher removal percentage.

Besides, the remaining variables ([NaH$_2$PO$_4$], [NaHCO$_3$], [NaNO$_3$], [Na$_2$SO$_4$], [HA]) have been excluded from the DSD model since they are statistically insignificant. These outcomes are reasonable since the effects of most anions on the oxidation performance are almost negligible, due to the low electrolyte concentration employed (<20 mM).[5] The only exception is chloride ion, which may be attributed to the enhanced generation of sulfate radicals ($^\bullet$SO$_4^-$) from PMS activation, as well as to the contribution of active chlorine (see eqn (3)–(9)).[23]

$$Co^{2+}(aq) + HSO_5^-(aq) \rightarrow Co^{3+}(aq) + {}^\bullet SO_4^-(aq) + OH^-(aq) \quad (3)$$

$${}^\bullet SO_4^-(aq) + OH^-(aq) \rightarrow {}^\bullet OH(aq) + SO_4^{2-}(aq) \quad (4)$$

$${}^\bullet SO_4^-(aq) + Cl^-(aq) \rightarrow {}^\bullet Cl(aq) + SO_4^{2-}(aq) \quad (5)$$

$${}^\bullet Cl(aq) + {}^\bullet Cl(aq) \rightarrow Cl_2(aq) \quad (6)$$

$$Cl_2(aq) + H_2O(l) \leftrightarrow HClO(aq) + H^+(aq) + Cl^-(aq) \quad (7)$$

$$Cl^-(aq) + HSO_5^-(aq) \rightarrow SO_4^{2-}(aq) + HClO(aq) \quad (8)$$

$$HSO_5^-(aq) + H^+(aq) + 2Cl^-(aq) \rightarrow SO_4^{2-}(aq) + H_2O(l) + Cl_2(aq) \quad (9)$$

Due to their high oxidation power, the active chlorine species generated quickly bleach AO II dye and accelerate the

Table 5 Independent variables of the CCRD experimental design

Level	X_1 [NaCl]: mM	X_2 [PMS]: mM	X_3 [Co^{2+}]: mM
−1.68	0	3.3	0
−1	6.8	6	0.29
0	16.8	10	0.71
+1	26.8	14	1.14
+1.68	33.6	16.7	1.42

degradation. Besides, our results indicate that there are no significant interactive effects between the anions, thus revealing the ion-selective nature of Co^{2+}/PMS system. In addition, [HA] also demonstrates weak effect toward AO II degradation for its low initial concentrations.

To achieve the maximum oxidation performance, we executed a five-level CCRD to further optimizations. Three significant variables ([NaCl], [PMS] and [Co^{2+}]) and their operating levels were shown in Table 5. In this design, [AO II] was set as 200 mg dm^{-3} and thus not being considered as a variable.

A total of 17 entries were performed randomly according to 3-factor CCRD. Table 6 presented the design matrix and the decolorization percentage of AO II at 60 min (Y_2, in %). Accordingly, a fitted second-order polynomial model with coded variables was constructed as follows:

$$Y_2 = 37.58 + 5.54X_1 + 6.98X_2 + 9.85X_3 + 3.78X_1X_2 - 0.34X_1X_3 + 0.11X_2X_3 - 0.15X_1^2 + 0.87X_2^2 + 0.47X_3^2 \quad (10)$$

As a result, the model F-value of 4.116 (>2.832) and the square regression coefficient (R^2) of 0.957 (>0.900), suggest a good agreement between predicted and actual responses.[24]

Based on eqn (10), we plotted the corresponding response surfaces (see Fig. 1). As expected, all variables still demonstrate
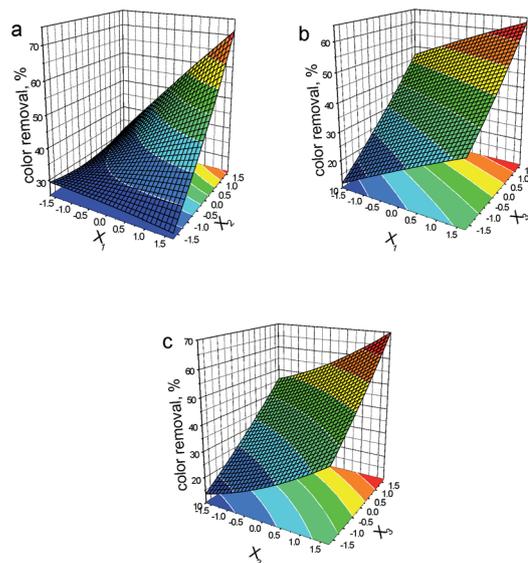
Table 6 Coded levels for the CCRD matrix used for RSM analysis of the chemical oxidation of AO II in Co^{2+}/PMS system. The response factor (Y_2) was obtained at 60 min of oxidation corresponding to AO II decolorization percentage (in %)

Entry	X_1	X_2	X_3	Y_2
1	−1	−1	−1	19.51
2	+1	−1	−1	26.58
3	−1	+1	−1	26.90
4	+1	+1	−1	50.39
5	−1	−1	+1	43.17
6	+1	−1	+1	50.15
7	−1	+1	+1	52.29
8	+1	+1	+1	73.12
9	−1.68	0	0	26.39
10	+1.68	0	0	36.66
11	0	−1.68	0	24.85
12	0	+1.68	0	43.93
13	0	0	−1.68	21.63
14	0	0	+1.68	44.93
15	0	0	0	38.46
16	0	0	0	38.15
17	0	0	0	38.07

Fig. 1 Response surfaces generated from the CCRD design using eqn (10) for color removal rate of AO II (X_1: [NaCl]; X_2: [PMS]; X_3: [Co^{2+}]).

positive effects on the oxidation performance, which are in line with those recorded in DSD model. Thus, the optimal process conditions for the last entry are: [NaCl] of 33.6 mM, [PMS] of 16.7 mM and [Co^{2+}] of 1.42 mM.

Fig. 2a depicts both color and TOC removal rates of the reaction medium under optimized operating conditions. The actual response (68.47 of Y_2) is in good agreement with predicted response (69.72), which has further confirmed the reliability of the model. Besides, a TOC removal rate of 49.6% following with a decolorization rate of 95.5% was achieved at 120 min, indicating the formation and accumulation of degraded products. To confirm this assumption, the corresponding UV-vis spectra during the oxidations are presented to extract some qualitative information concerning the changes of AO II molecules. As depicted in Fig. 2b, the spectrum of AO II presents an absorption peak in the visible region (λ_{max} 485 nm) which is responsible for the orange color of the dye. The bands in the UV region mainly arise from the $\pi \rightarrow \pi^*$ transitions of the aromatic structures: in particular, the sharp peaks at 311 nm and 236 nm may be assigned to the naphthyl ring and phenyl ring of AO II, respectively.[25] Although these three absorption peaks all decreased continuously during the treatment, a new peak appears at 262 nm. This phenomenon indicates that some refractory intermediates are generated during the oxidations, which have been identified by the following analyses.

3.2. Mechanistic study

The degradation mechanisms of AO II in •OH-based technologies (e.g., TiO$_2$ photocatalysis and electrochemical oxidation) have been well investigated in previous studies.[26–28] However, little work is conducted concerning the oxidation pathways of organics in •SO$_4^−$-based processes. Unlike •OH, •SO$_4^−$ and Cl$_2$ are assumed to react with organics through electron transfer
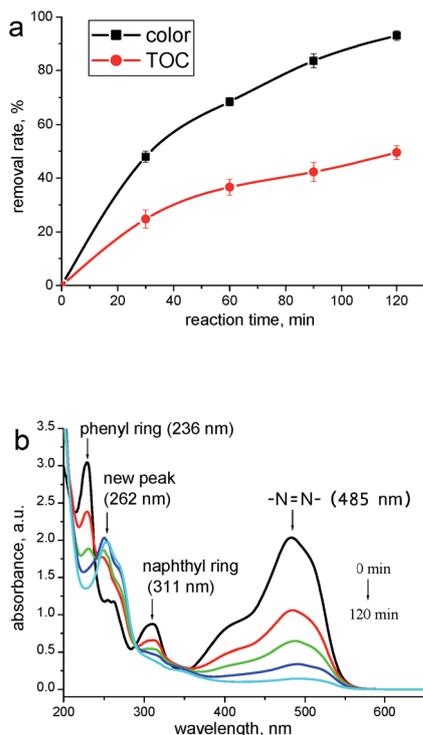
Fig. 2 (a) Comparison of color and TOC removal efficiency with reaction time under the optimum conditions established by RSM; (b) temporal absorbance variation of UV-vis of AO II during *in situ* chemical oxidation in Co^{2+}/PMS system (dilution ratio: 5).

Fig. 3 Charge densities of the atoms in the molecule of AO II (excluding H atoms).

mechanism, which makes them more selective than $\cdot$OH.[4] Thus, we attempted to elucidate the reaction pathway of AO II in Co^{2+}/PMS/Cl⁻ system.

Before studying the degraded products, quantum chemistry calculations were conducted to clarify the oxidation behavior of AO II dye. The charge densities of atoms in pollutant molecule offered important information on the reaction sites.[29] Hence, using density functional theory (DFT) in ChemBio3D software package, the charge densities of the atoms in AO II molecule were calculated after minimizing the energy (see Fig. 3). By comparing the charge densities of the neighboring atoms, three active sites in AO II molecule had been successfully identified (*i.e.* I: C(2)–S(20) bond; II: C(5)–N(7) bond; III: C(9)–N(8) bond). In other words, these bonds were more prone to rupture than other bonds during the chemical oxidations, as a result of their marked differences concerning the neighboring charge densities.

To confirm the hypothesis, the major intermediates formed during the oxidations were identified using LC/MS technique. Briefly, this analysis permitted the identification of sixteen main intermediates, compounds with *m/z* value of 94, 110, 111, 128, 128, 146, 158, 161, 162, 166, 179, 180, 214, 248, 249 and 264 (see Fig. 4). The structures of intermediates were proposed on the basis of the exact mass of pseudo-molecular ions in the MS spectra plus the interpretation of MS patterns. Judging from the structural characteristics, these intermediates may be classified into three types: desulfonated products of AO II (**1** and **2**), derivatives of phenol (**3, 4, 7, 8, 12, 13** and **16**) and derivatives of
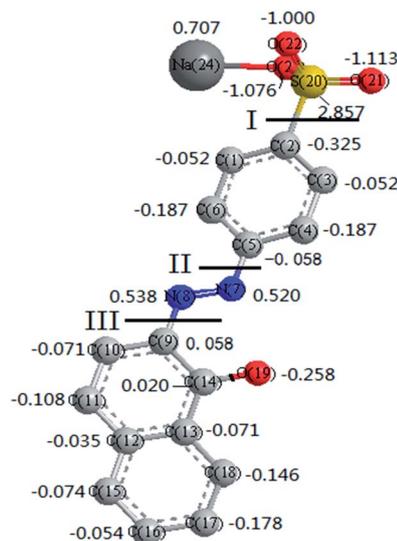
naphthol (**5, 6, 9, 10, 11, 14** and **15**). Their formations indicate the breakage of C–N bond, as well as the substitution of *ortho*- and *para*-positions of phenol and naphthol rings. These outcomes are in well accordance with those obtained from theoretical analyses.

Based on the above, the proposed oxidation pathways of AO II in Co^{2+}/PMS/Cl⁻ system are shown schematically in Fig. 4. According to the sequence, three kinds of reactive agents are probably involved are: $\cdot SO_4^-$, Cl_2 and $\cdot$OH. In the presence of these oxidants, the AO II degradation is assumed to follow oxidation pathway leading to hydroxylated and chlorinated
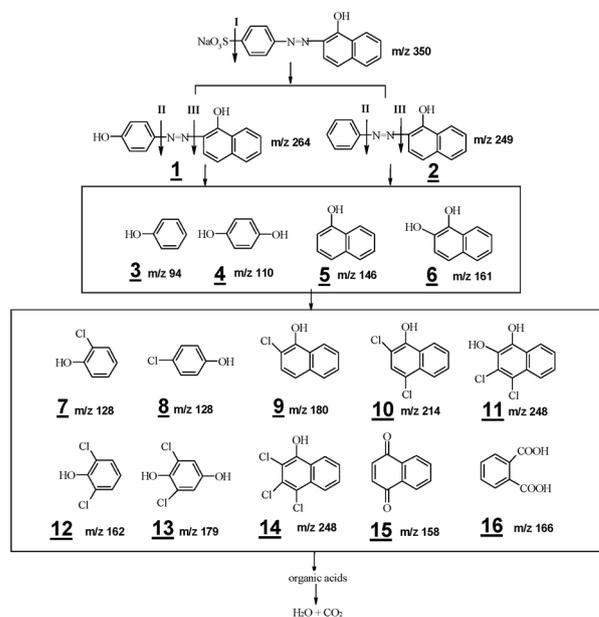

Fig. 4 Proposed reaction pathway for the oxidation of AO II by Co^{2+}/PMS/Cl⁻ system.

intermediates, plus C–N and C–S cleavage products through competitive routes. Particularly, active chlorine attacks at the *ortho*- and *para*-positions of phenol and naphthol result in the formation of aromatic chlorohydrocarbon (electrophilic substitution reactions). The oxidation process continues with a breakage of aromatic rings, resulting in the production of carboxylic acids.[30] With prolonged reaction time, these organic acids continue reacting until they turn into CO_2 and H_2O. Despite this, the comprehensive transformation map of chloride ions in Co^{2+}/PMS system should be carefully examined before such technology is used to eliminate organic pollutants in real practice.

4. Conclusions

The *in situ* chemical oxidation of AO II by homogeneous Co^{2+}/PMS system was initially studied by adopting a sequential experimental strategy consisting of a screening phase (DSD) followed by a optimizing phase (CCRD). The main conclusions of the work were the following:

(1) It had been realized that both DSD and CCRD models are reliable and predictive tools with excellent accuracy. Thus, the strategy (DSD plus CCRD) was highly recommended for process optimizations, especially for processes involving large number of operating parameters;

(2) Among the anions adopted, only chloride ions displayed significant roles during the chemical oxidations. The ion-selective nature of Co^{2+}/PMS system was thus successfully identified.

(3) Optimum degradation of AO II was achieved by applying [NaCl] of 33.6 mM, [PMS] of 16.7 mM and [Co^{2+}] of 1.42 mM, being reduced color by 95.5% and TOC by 49.6% (for [AO II] of 200 mg dm^{-3});

(4) The oxidation of AO II in Co^{2+}/PMS/Cl^- system was found to lead to the formation of chlorinated and non-chlorinated aromatics. This implied that, besides sulfate radicals, active chlorine species also participated in the oxidation processes. It was thus reasonable to conclude that for the current system, the presence of chlorides not only affected the degradation kinetics but also the pathways and mechanisms through which the oxidation occurred.

(5) Considering the possible environmental risks, the fate and role of chloride ions in Co^{2+}/PMS system should be extensively examined before any real applications. Further works are recommended to be put forward in this field.

Conflicts of interest

There are no conflicts to declare.

Acknowledgements

References

1 J. M. Monteagudo, A. Durán, R. González and A. J. Expósito, *Appl. Catal., B*, 2015, **176–177**, 120–129.
2 J. Sharma, I. M. Mishra, D. D. Dionysiou and V. Kumar, *Chem. Eng. J.*, 2015, **276**, 193–204.
3 J. Cong, G. Wen, T. Huang, L. Deng and J. Ma, *Chem. Eng. J.*, 2015, **264**, 399–403.
4 Y. Ji, C. Dong, D. Kong and J. Lu, *J. Hazard. Mater.*, 2015, **285**, 491–500.
5 P. Hu and M. Long, *Appl. Catal., B*, 2016, **181**, 103–117.
6 S. L. C. Ferreira, R. E. Bruns, E. G. P. Silva, W. N. L. Santos, C. M. Quintella, J. M. David, J. B. Andrade, M. C. Breitkreitz, I. C. S. F. Jardim and B. B. Neto, *J. Chromatogr. A*, 2007, **115**, 2–14.
7 E. Chatzisymeon, N. P. Xekoukoulotakis, E. Diamadopoulos, A. Katsaounis and D. Mantzavinos, *Water Res.*, 2009, **43**, 3999–4009.
8 C. Zhang, J. Wang, H. Zhou, D. Fu and Z. Gu, *Chem. Eng. J.*, 2010, **161**, 93–98.
9 E. Petrucci, L. D. Palma, R. Lavecchia and A. Zuorro, *J. Taiwan Inst. Chem. Eng.*, 2015, **51**, 152–158.
10 S. D. Georgiou, S. Stylianou and M. Aggarwal, *Statistics*, 2014, **48**, 815–833.
11 S. D. Priyadharshini and A. K. Bakthavatsalam, *Bioresour. Technol.*, 2016, **207**, 150–156.
12 B. Jones and C. J. Nachtsheim, *J. Qual. Technol.*, 2013, **43**, 1–15.
13 M. Fidaleo, R. Larecchia, E. Petrucci and A. Zuorro, *Int. J. Environ. Sci. Technol.*, 2016, **13**, 835–842.
14 E. S. Hecht, J. P. McCord and D. C. Muddiman, *Anal. Chem.*, 2015, **87**, 7305–7312.
15 K. J. Kauffman, D. G. Dorkin, J. H. Yang, M. W. Heartlein, F. DeRosa, F. F. Mir, O. S. Fenton and D. G. Anderson, *Nano Lett.*, 2015, **15**, 7300–7306.
16 W. Libbrecht, F. Deruyck, H. Poelma, A. Verberckmoes, J. Thybaut, J. D. Clercq and P. V. D. Voort, *Chem. Eng. J.*, 2015, **259**, 126–134.
17 X. Du, Z. Zhang, C. Zhang and D. Fu, *Chemosphere*, 2017, **171**, 362–369.
18 S. Bajpai, S. K. Gupta, A. Dey, M. K. Jha, V. Bajpai, S. Joshi and A. Gupta, *J. Hazard. Mater.*, 2012, **227–228**, 436–444.
19 C. Zhang, L. Yang, F. Rong, D. Fu and Z. Gu, *Electrochim. Acta*, 2012, **64**, 100–109.
20 F. Qi, W. Chu and B. Xu, *Appl. Catal., B*, 2013, **134–135**, 324–332.
21 F. Qi, W. Chu and B. Xu, *Chem. Eng. J.*, 2014, **235**, 10–18.
22 C. Zhang, L. Liu, W. Li, J. Wu, F. Rong and D. Fu, *J. Electroanal. Chem.*, 2014, **726**, 77–83.
23 Z. Wang, R. Yuan, Y. Guo, L. Xu and J. Liu, *J. Hazard. Mater.*, 2011, **190**, 1083–1087.
24 L. C. Almeida, S. Garcia-Segura, N. Bocchi and E. Brillas, *Appl. Catal., B*, 2011, **103**, 21–30.

25 J. Hastie, D. Bejan and M. N. J. Bunce, *Ind. Eng. Chem. Res.*, 2006, **45**, 4898–4904.

26 J. Qu and X. Zhao, *Environ. Sci. Technol.*, 2008, **42**, 4934–4939.

27 O. Scialdone, A. Galia and S. Sabatino, *Appl. Catal., B*, 2014, **148–149**, 473–483.

28 E. Kusmierek and E. Chrzescijanska, *J. Photochem. Photobiol., A*, 2015, **302**, 59–68.

29 Y. Lei, G. Zhao, Y. Zhang, M. Liu, L. Liu, B. Lv and J. Gao, *Environ. Sci. Technol.*, 2010, **44**, 7921–7927.

30 L. Chen, P. Campo and M. J. Kupferle, *J. Hazard. Mater.*, 2015, **283**, 574–581.